SWU Engineering Journal (2018) 13(1), 132-142 วารสารวิศวกรรมศาสตร์ มหาวิทยาลัยศรีนครินทรวิโรฒ
ปีที่ 13 ฉบับที่ 1 เดือนมกราคม – เมษายน พ.ศ. 2561

A Unique Grid-flux-oriented Control Algorithm for Synchronization and Power Controls of a Doubly-Fed Induction Generator System

Sutthimat Mueangngoen and Yuttana Kumsuwan*
Department of Electrical Engineering, Faculty of Engineering,Chiang Mai University
Chiang Mai, Thailand, 50200
* Corresponding author: E-mail: yt@eng.cmu.ac.th

ABSTRACT

This paper presents a synchronization method and the power control by using a grid-flux-oriented control (GFOC) algorithm for a two-level back-to-back converter fed doubly-fed induction generator (DFIG) system. Here, the synchronization process and power control with toque/speed modes of the generator are controlled by a unique rotor current control. Based on the GFOC algorithm for the regulation of the stator magnetizing current, the exciting component of the rotor current is fully controlled, and the variation of the subsynchronous, synchronous, and supersynchronous speed is controlled by the torque component of the rotor current for the stator power control. The excellent performance of the proposed GFOC algorithm with DFIG drive is verified through the simulation results considering the DFIG as connected/disconnected to ac mains, and torque/speed-control modes.

Keyword: Doubly-fed induction generator (DFIG), grid-flux-oriented control (GFOC), synchronization process.

1. Introduction

Doubly-fed induction generator (DFIG) systems are extensively applied in wind power conversion due to the desirable synchronous generator operation at a lower cost [1]-[6]. Moreover, the four-quadrant power control is able to operate with the 25-30 % back-to-back converter installation of the rated generator power. The flexible operation with the variable speed and constant frequency under the subsynchronous, synchronous, and supersynchronous modes has been attractive in this system.

Regarding the synchronization process and the power control for the DFIG systems, there are three main groups of vector current controls for the rotor-side converter [1] ,[6] - [10] ,[11] as follows: 1) The stator-flux-oriented control (SFOC), 2) The stator voltage oriented control (SVOC), and 3) The grid-flux-oriented power control (GFOC). In [1], this scheme uses the stator-flux vector reference frame to independently control the active and reactive powers. However, this proposed control requires a low-pass filter to estimate the stator-flux position which leads to small offsets/dc drift and saturation problems. The SVOC is used for the DFIG in [6].

This method needs to calculate only the stator voltage position, which is easy to be directly estimated by measuring the stator voltage. Because the stator flux position is not respected, the SVOC may not support the synchronization process. In [11], this algorithm employs the grid voltage to form the virtual grid-flux position for the control of the stator-flux vector without the stator-flux estimation. Among these literatures, they are still unclear about the synchronization process, which is very important for the starting operation in order to further control the overall system.

A few literatures have been reported and analyzed the comprehensive synchronization process with the power controls. In [1], the synchronization with the SFOC method is carried out by a direct on line starting operation. The extraction of the reactive power leads to the inrush stator current and the poor power factor at the utility grid. To discard such the drawbacks, the synchronization before the grid-connected process based on the SFOC method is proposed in [6]-[10]. However, the PI controller is consumed in this process. It affects a slack dynamic response and adds a complicated controller design. In [11], the GFOC algorithm based on the mathematical synthesis of the stator-flux position is firstly presented for the synchronization process, whereas the SFOC algorithm is separately applied for the power control operation. Based on two control algorithms, it does not involve a simple software implementation approach.

In this paper, a unique one-stage model for the synchronization and power control in a DFIG system based on a GFOC algorithm is proposed. The different characteristics of the proposed GFOC algorithm are summarized as follows:

1) One- stage GFOC algorithm for the synchronization process and the power controls simplifies the procedure of the implementation and the controller design from [11].

2) Unlike [6]-[10], the estimation of the stator-flux position using the low- pass filter is not necessary. The problems of the filter saturation and the dc drift can be accordingly overcome.

3) The better dynamic performance is achieved without delay of the achievable stator-flux position when compared to [6]. Additionally, it can be ensured that the inrush current stator current does not appear compared to [1].

According to the salient features, the dynamic and steady- state simulation results are demonstrated to verify the performance of the proposed control algorithm for the DFIG system.

2. Dynamic Model of Doubly-Fed Induction Generator

The configuration of the DFIG system is shown in Fig. 1. The stator of the generator can be directly connected to the grid whereas the rotor circuit is connected to the grid through a back-to-back converter, which consisted of rotor-side converter and grid-side converter. Thus, in order to analyze the performance of the proposed GFOC algorithm in the next section, the space vector voltage and flux equations of the DFIG in synchronous rotating frame can be expressed as [1].

$$\vec{v}_s = R_s \vec{i}_s + \frac{d\vec{\lambda}_s}{dt} + j\omega_s \vec{\lambda}_s \qquad (1)$$

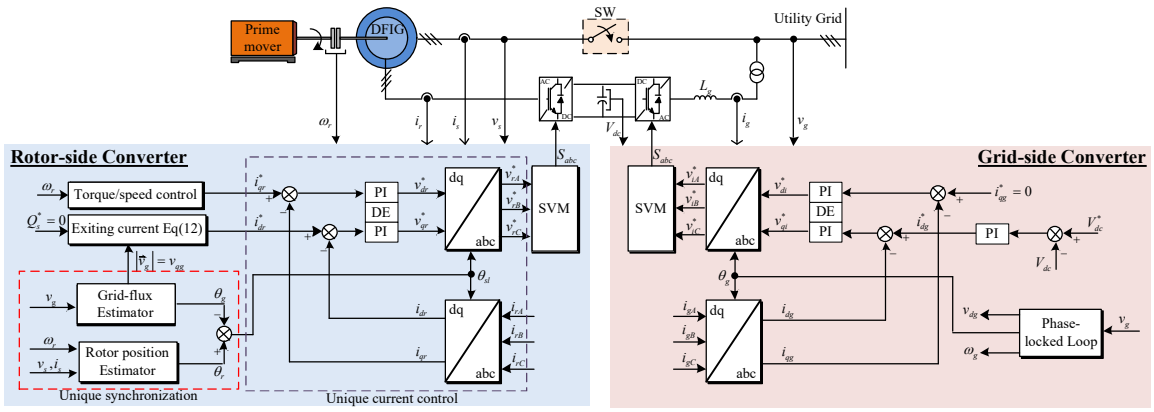

Fig. 1 Synchronization and control diagram of rotor-side converter with GFOC algorithm.

$$\vec{v}_r = R_r\vec{i}_r + \frac{d\vec{\lambda}_r}{dt} + j\omega_{sl}\vec{\lambda}_r \quad (2)$$

$$\vec{\lambda}_s = L_s\vec{i}_s + L_m\vec{i}_r \quad (3)$$

$$\vec{\lambda}_r = L_r\vec{i}_r + L_m\vec{i}_s \quad (4)$$

where R_s, R_r are the stator and rotor resistances, L_s, L_r are the self-stator and –rotor inductances, L_m is the magnetizing inductance, and $\omega_s, \omega_r, \omega_{sl}$ are the synchronous, rotor and slip angular speeds, respectively.

The electromagnetic torque of the DFIG is given by

$$T_e = \frac{3}{2}P_p\left(\lambda_{ds}i_{qs} - \lambda_{qs}i_{ds}\right) \quad (5)$$

where T_e is the electromagnetic torque and P_p is the pole pairs.

The active power and reactive power of the DFIG, where the power loss in stator side can be neglected, are calculated by

$$P_s = \frac{3}{2}\left(v_{ds}i_{ds} + v_{qs}i_{qs}\right), \quad (6)$$

$$Q_s = \frac{3}{2}\left(v_{qs}i_{ds} - v_{ds}i_{qs}\right) \quad (7)$$

where P_s, Q_s are the active power and the reactive powers, respectively.

3. Proposed GFOC Algorithm

In this section, the proposed GFOC algorithm is applied for the rotor-side converter to achieve the synchronization and power control processes. It can be shown in the

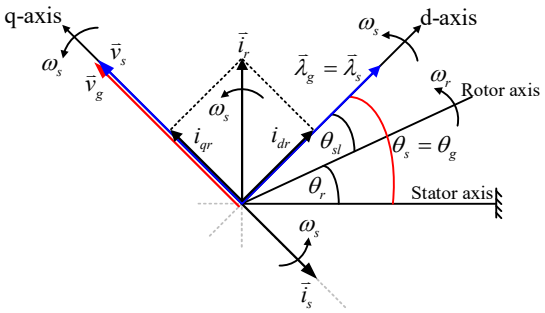

Fig. 2 Space vector phasor of the DFIG with GFOC.

block diagram of the GFOC algorithm (see the rotor-side converter control), as shown in Fig. 1. With the unique synchronization for beginning, as shown in the red dash line border, one of two block diagrams is to estimate the magnitude of grid voltage $|v_g|$ and grid-flux position θ_g, called "Grid flux Estimator", and another block diagram is to calculate the correct rotor position (θ_r), called "Rotor position Estimator". Using grid-flux

and rotor positions, the correct slip position (θ_{sl}) is then achieved to further use for the reference frame transition in "the unique current control (UCC)". In the UCC, as shown in black dash line border, it is to control the rotor current for synchronization and power control process corresponding to unique synchronization process. Besides, the grid-side converter has the conventional control scheme [12] to regulate the dc-link and exchange the power between the grid and generator.

A. Unique Synchronization Process

In order to always be synchronized with the grid all of the operations, a unique synchronization with GFOC is realized in this paper. Fig. 2 shows the space vector phasor of the DFIG with the proposed control. The grid voltage vector is aligned to of the rotating reference frame and perpendicular to the virtual grid flux vector, which is located on the with the grid flux position. For the synchronization process, the stator flux vector controlled through the magnetizing stator current can be obtained by

$$\left|\vec{\lambda}_g\right| = \lambda_{dg} = \lambda_{ds} = L_m i_{ms} \ , \ \ \lambda_{qg} = \lambda_{qs} = 0. \qquad (8)$$

Therefore, the induced stator voltage vector $\vec{v}_s$ can be synchronized with the grid voltage vector $\vec{v}_g$ as follows

$$\left|\vec{v}_g\right| = v_{qg} = v_{qs} \quad , \quad v_{dg} = v_{ds} = 0. \qquad (9)$$

$$\theta_g = \theta_s = \theta_r + \theta_{sl} \qquad (10)$$

where $\theta_s, \theta_r, \theta_{sl}$ are the stator flux, the rotor position and the slip angle, respectively. The correct slip angle for a unique synchronization is calculated by the virtual grid flux position θ_g as follow

$$\theta_{sl} = \theta_g - \theta_r. \qquad (11)$$

From (8)-(11), the correct slip angle θ_{sl} is directly provided by the virtual grid- flux position θ_g that leads to the one- stage algorithm for synchronization process, grid connected/ disconnected and stator power controls. Thus, the stator voltage vector $\vec{v}_s$ is completely synchronized with the grid voltage vector $\vec{v}_g$, and it can be shown the control block at the red dashed line in Fig. 1. In addition, the rotor current components i_{dr}, i_{qr}, which produce the induced stator voltage and electromagnetic torque, respectively, will be described in the next section.

B. Unique Rotor Current Control

Initially, the system is not connected to the grid, the stator current is still zero $i_s = 0$. Based on steady-state conditions, from (1)-(4) and (7), the d-axis rotor current can be written by

$$i_{dr} = -\frac{2}{3}\frac{L_s}{v_{qs} L_m} Q_s + \left|\vec{i}_{ms}\right|. \qquad (12)$$

From (12), for the unity power factor operation, the reference stator reactive power Q_s^* is set to zero. Thus, the d-axis reference rotor current or the reference exciting rotor current i_{dr}^*, which is proportional to the induced stator voltage, can be determined by the q-axis grid voltage v_{qg} as the following

$$i_{dr}^* = \left|\vec{i}_{ms}\right| = \frac{v_{qg}}{\omega_s L_m}. \qquad (13)$$

From the above equation, it can be seen that the exciting rotor current i_{dr}^{*} is constantly equal to the stator magnetizing current vector $\vec{i}_{ms}$, which produces the stator flux and aligns with the virtual grid flux. For this reason, the value of stator voltage is directly controlled by the q-axis grid voltage v_{qg}.

After the system is synchronized and connected to the grid, the stator power can be delivered to the grid by the command torque rotor current i_{qr}^{*}, which is determined from (5) and (6), as the following

$$i_{qr}^{*} = \frac{2}{3}\frac{\omega_s L_s}{P_p L_m v_{qg}} T_e^{*}. \qquad (14)$$

From (14), it can be observed that the reference electromagnetic torque T_e^{*}, which is commanded by the torque control or the speed control algorithm [12], is proportional to the reference torque rotor current i_{qr}^{*}. In Fig. 2, when the torque rotor current i_{qr} is activated, the stator current vector $\vec{i}_s$ appears at q-axis of the reference frame causes the DFIG to supply active power to the grid. Overall, a unique current control is shown by the purple dashed line in Fig. 1. That means the proposed GFOC algorithm is controlling for the synchronization and the power control process in one-stage, based on only the grid-side.

4. Simulation Results

The simulated dynamic and steady-state performance of the proposed GFOC algorithm for the two-level back-to-back converter fed DFIG drive is carried out using MATLAB/Simulink software. The testing procedure of the proposed system consisted of the grid-connected/ disconnected synchronization along with torque control and speed control modes under the condition of a rotor speed variation of 1200 to 1800 rpm. For the test system, PI controller for the current controls of rotor-side and grid-side converters are designed following [1]. The convenient parameters of the DFIG can be shown in Table 1.

TABLE I
DFIG Parameters, which is produced by Lucas Nulle, Germany

Variable	Parameters	Value	
v_s, v_r	Rated stator and rotor voltage	380,127	V
$i_{s,peak}$	Rated peak stator current	2.1	A
$P_{s,rated}$	Rated stator power	1.0	kW
$T_{e,rated}$	Rated electromagnetic torque	6.3	Nm
R_s	Stator resistance per phase	7.9	Ω
R_r	Rotor resistance per phase	8.8	Ω
L_s, L_r	Stator and rotor inductance	0.78	H
L_m	Magnetizing inductance	0.70	H
P_p	Number of Pole pairs	2	
$N_s : N_r$	Stator and rotor Ratio	1.732	
Back-to-back converter and utility grid parameters			
v_g, f_g	Utility grid voltage and frequency	380/50	V/Hz
V_{dc}	Nominal dc-link voltage	180	V
C_{dc}	Dc-link capacitor	1625	μF
f_{sw}	Switching frequency	4	kHz

A. Operation of Doubly-Fed Induction Generator System with torque control mode

Fig. 3 shows the simulation results for the proposed GFOC in the torque control mode. The dynamic and steady- state performances of the synchronization process, grid-connected/disconnected, and stator power control are reported in Fig. 3(a)-(d), in terms of the reference rotor current along with the

actual rotor currents , the three-phase rotor current along with the rotor speed, the stator and grid voltage, and the stator current, respectively.

It can be described in four scenarios as follows:

1) In period □ (t = 0.02 – 0.10 s): The speed of the generator is initially in the subsynchronous speed at 1200 rpm. At t = 0.02 s, the reference exciting rotor current is changed by a step command from the lacking induction to the rated value according to (13), whereas both the reference torque rotor current and the actual torque rotor current are equal to zero. Therefore, the actual exciting rotor current is linearly conducted until its rated value at

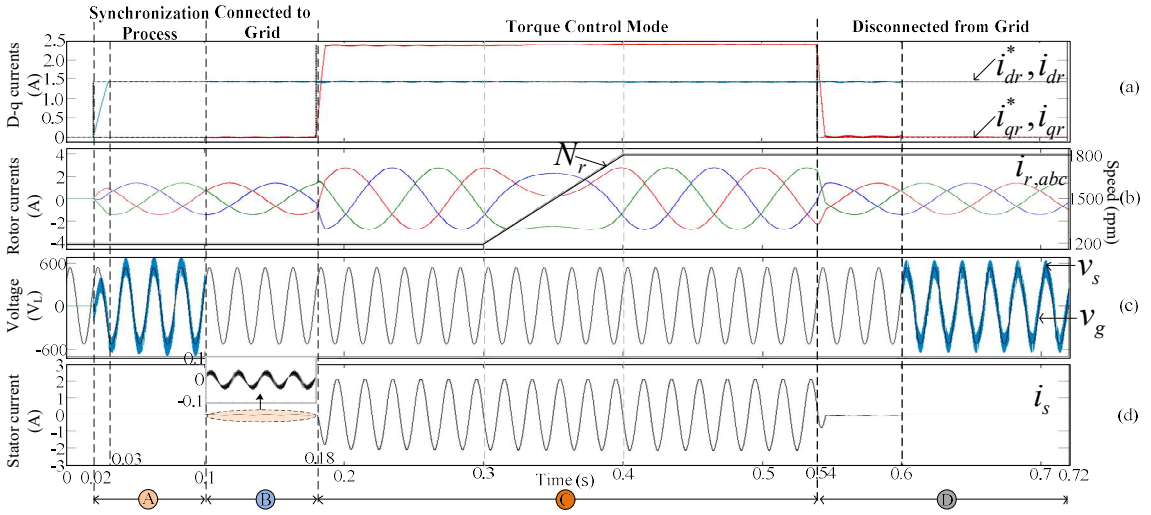

Fig. 3 Simulation results for the proposed GFOC algorithm with torque control mode. (a) Rotor currents. (b) Three-phase rotor currents and speed. (c) Stator and grid line-to-line voltages. (d) Phase stator current.

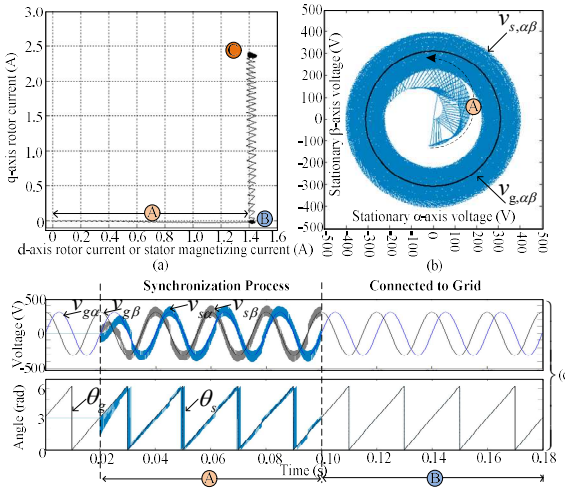

Fig. 4 Synchronization and power control operation of Fig. 3. (a) XY plot of the rotor currents. (b) Trajectory of the stator and grid voltages. (c) Phase stator and grid voltages and its position angles.

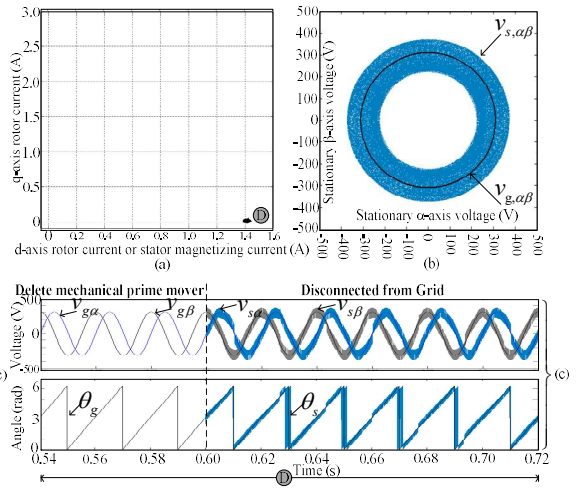

Fig. 5 Disconnection operation of Fig. 3. (a) XY plot of the rotor currents. (b) Trajectory of the stator and grid voltages. (c) Phase stator and grid voltages and its position angles.

t = 0.03 s. This leads to the corresponding increment of the three-phase rotor current. The stator line-to-line voltage is then induced and completely synchronized into the grid voltage, whereas the stator current is still zero.

2) In period □ (t = 0.10 – 0.18 s): The stator terminal is directly connected to the grid at t = 0.10 s. It can be seen that the actual exciting rotor current and the three-phase rotor current can be regulated at the rated value. Hence, the stator voltage fully becomes the grid voltage with the negligible stator current at 2% of its rated value, without the effect of the inrush current. This can confirm the smooth grid-connected of the proposed system.

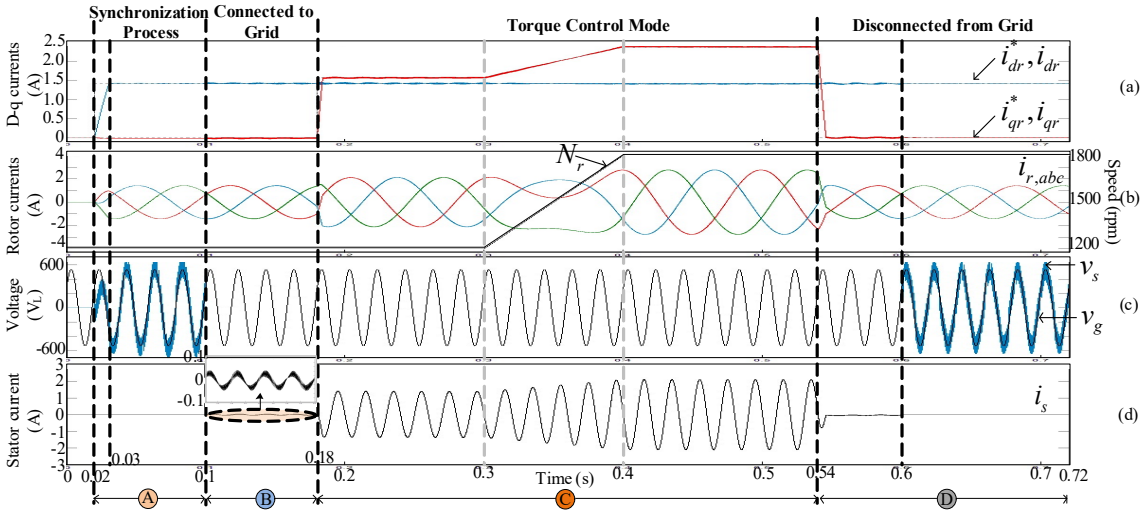

Fig. 6 Simulation results for the proposed GFOC algorithm with speed control mode. (a) Rotor currents. (b) Three-phase rotor currents and speed. (c) Stator and grid line-to-line voltages. (d) Phase stator current.

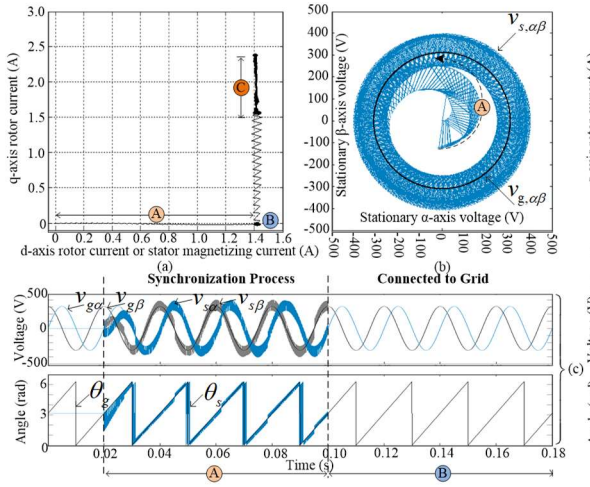

Fig. 7 Synchronization and power control operation of Fig. 6. (a) XY plot of the rotor currents. (b) Trajectory of the stator and grid voltages. (c) Phase stator and grid voltages and its position angles.

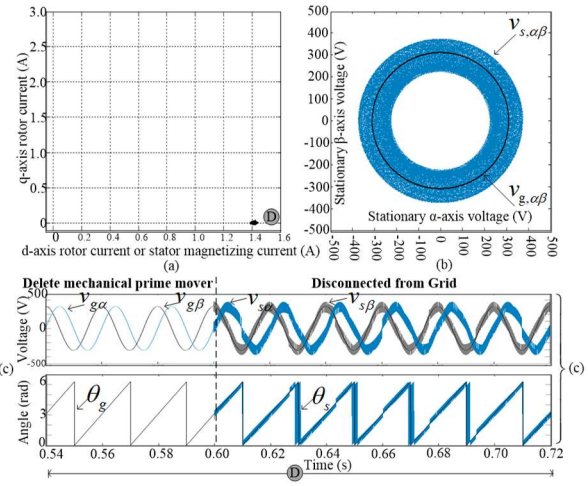

Fig. 8 Disconnection operation of Fig. 6. (a) XY plot of the rotor currents. (b) Trajectory of the stator and grid voltages. (c) Phase stator and grid voltages and its position angles.

3) In period □ (t = 0.18 – 0.54 s): The electromagnetic torque control begins by the sudden step up of the reference torque rotor current to the rated value, which leads to a constant electromagnetic torque according to (14). Meanwhile, although the rotor speed is changed from subsynchronous speed (1200 rpm) to supersynchrnous speed (1800 rpm), the actual torque rotor current is still kept constant, as expected, unless the phase sequence of the three- phase rotor current is inverse. In addition, the desired stator voltage and current are maintained by the torque control mode. This is pointed out to the

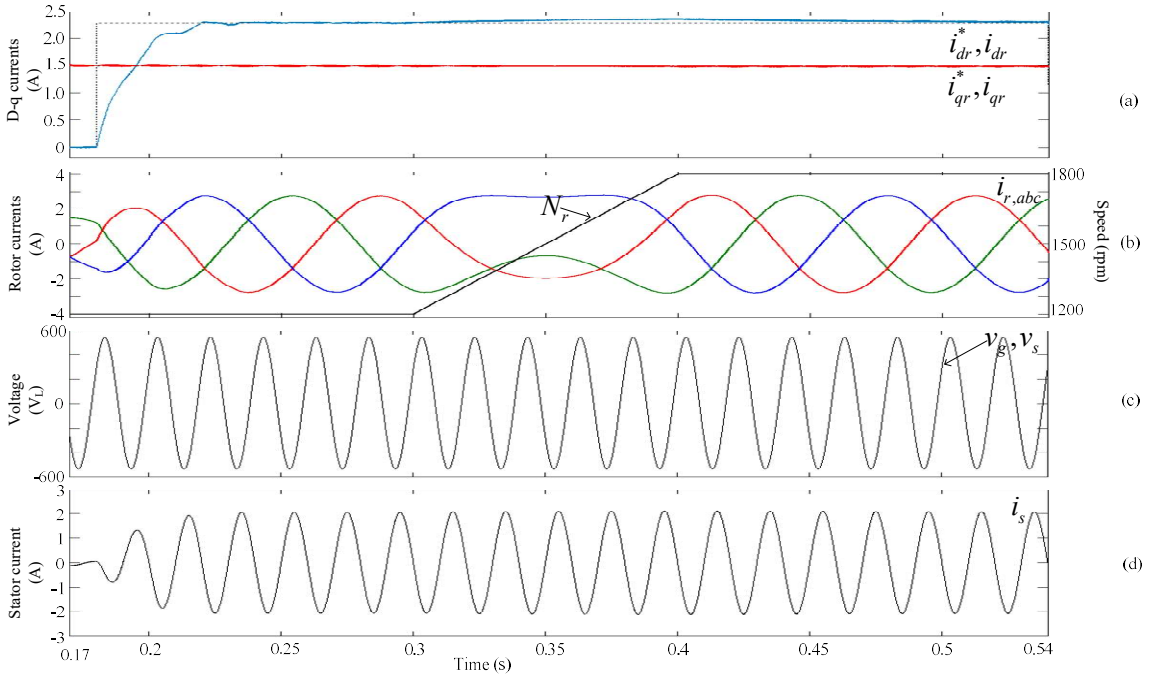

Fig. 9 Simulation results of power control for DFIG using SVOC [6]. (a) Rotor currents. (b) Three-phase rotor currents and speed. (c) Stator and grid line-to-line voltages. (d) Phase stator current.

stable performance of the proposed control algorithm.

4) In period □ (t = 0.54 – 0.72 s): Finally, in order to disconnect the system in the decrease the electromagnetic torque to zero. For this reason, the stator current is immediately reduced to zero. Meanwhile, the three-phase rotor current is decreased from the rated value to its excited value, but it does not impact on the stator voltage due to the actual exciting rotor current is kept constant. The utility grid disconnection is carefully succeeded at t = 0.60 s without the inrush current, in spite of the remaining induced stator voltage and with the existing synchronization.

Fig. 4 shows the dynamic operation of the synchronization process. The xy plot of the actual rotor excitation current is changed from the origin

point to its excited value point corresponding to its waveforms of Fig. 3(a) in period □, as shown in Fig. 4(a). Simultaneously, it can be observed that the phase stator voltage is induced and swirly in order to reach the trajectory of the phase grid voltage, as shown in Fig 4(b), according to their time domain along with the waveforms of the induced stator-flux position aligning the grid-flux position shown in Fig. 4(c). For the grid-parallel connection in period □ (see Fig. 3), the phase components of stator voltage are identical to those of the grid voltage for both magnitude and position views (see the black line in Fig. 4(b)), in accordance with the waveforms of Fig. 4(c). Then, the torque control operation corresponding to period □ of Fig. 3 is pointed out by the actual torque current component that perpendicularly racks into its rated value, as shown in Fig 4(a).

Fig. 5 shows the dynamic operation of the disconnection process. The xy plot of the actual torque current component is changed to zero, whereas the actual rotor excitation current still stands at its excited value, as shown in Fig. 5(a) and corresponding to Fig. 3 in period □. In Fig. 5(b), the phase stator voltage returns to be enclosed by the ripple while its trajectory is still synchronized, which is also visible from its component and position waveforms, as shown in Fig. 5(c).

B. Operation of Doubly- Fed Induction Generator System with speed control mode

Fig. 6 shows the simulation results for the proposed GFOC with the speed control mode. The response and performance resemble the previous results of the torque control mode (see in Fig. 3). However, after the system is synchronized and connected to the grid, the speed control leads to inconstant electromagnetic torque according to the rotor speed variation, as shown in Figs. 6(a) and 6(b) for period □. Moreover, the stator current is accordingly increased and proportional to torque rotor current, as shown in Fig. 6(d). In the same way, the dynamic operation results from the synchronization process in Fig. 7 are similar to Fig. 4, except that the electromagnetic torque is changeable in the speed control process. The xy plot of the actual torque rotor current gradually raise from the subsynchronous to supersynchronous speed with a lower error due to the linear change of the rotor speed, as shown in Fig. 7(a) for period □. Besides, the dynamic operation of the disconnection process of Fig. 8 has the same results as Fig. 5. As the results in section IV- A and – B, the proposed algorithm works as expected and proves its performance in both power control modes.

Compared with the existing SVOC method in [6], Fig. 9 shows the simulation results of power control for DFIG using SVOC method. In term of the results of Figs. 9(b)-(d), they are well in line with the proposed GFOC algorithm (see Figs. 3(b)-(d)). Unless, the $dq-axis$ rotor currents in Fig. 9(a) are different from the $dq-axis$ rotor currents in Fig. 3(a) due to its SVOC algorithm. This can guarantee that the power control performance of the proposed GFOC algorithm for

DFIG system is equivalent to the conventional SVOC method [6].

5. Conclusion

In this paper, the grid-flux-oriented control (GFOC) algorithm has been applied and confirmed for the synchronization process and power control process of the DFIG system. A unique synchronization and current rotor control process have been explained with equations in order to directly regulate the stator magnetizing current, or the exciting rotor current, for the induction of stator voltage and to fully control the electromagnetic torque for the power control process. With this algorithm, all of operation is controlled by the grid- side information based on one-stage synchronization. The dynamic simulation results can verify the performance operation of the DFIG under GFOC in the details as follows: 1) the DFIG is smoothly connected to the grid without the inrush current, 2) The power process can effectively operate with torque control and speed control under the variation of the subsynchronous, synchronous and supersynchronous speed mode, 3) All operations are controlled only by the GFOC algorithm.

6. References

[1] R. Pena, J. C. Clare, and G. M. Asher, “Doubly fed induction generator using back-to-back PWM converters and its application to variable speed wind-energy generation”, IEE Proc. Elec. Power Appl., vol. 143, no. 3, pp. 231-241, 1996.

[2] P. Vas, *Vector Control of AC Machines*. New York, Oxford Univ. Press, 1990.

[3] W. Leonhard, Control of Electrical Drives. Berlin, Springer Verlag 2001.

[4] S. Muller, M. Deicke, and R. W. De Doncker, “Doubly fed induction generator systems for wind turbines,” IEEE Ind. Appl. Mag., vol. 3, pp. 26–33, May/Jun. 2002.

[5] S. Z. Chen, N. C. Cheung,Y. Z., M. Zhang, and X. M. Tang, “Improved grid synchronization control of doubly fed induction generator under unbalanced grid voltage,” IEEE Trans. Energy Convers., vol. 26, no. 3, pp. 799-810, 2011.

[6] B. Wu, Y. Lang, N. Zargari, and S. Kouro, "Doubly fed induction generator based WECS," in Power Conversion and Control of Wind Energy Systems, New Jersey: Wiley-IEEE Press, 2011, pp.480-485.

[7] J. W. Park, K. W. Lee, D. W. Kim, K. S. Lee, and J. S. Park, “Control method of a doubly-fed induction generator with a grid synchronization against parameter variation and encoder position”, in Industry Applications Annual Meeting, New Orleans, LA., 2007, pp. 931-935.

[8] A. G. A. Khalil, D. C. Lee, and S. H. Lee, “Grid connection of doubly-fed induction generators in wind energy conversion system,” in International Power Electronics and Motion Control Conference, Shanghai, 2006, pp. 1-5.

[9] D. Yazdani, M. Pahlevaninezhad, and A. Bakhshai, “Three-phase grid synchronization techniques for grid connected converters in distributed generation systems,” in IEEE

International Symposium on Industrial Electronics, Seoul, 2009, pp. 1105- 1110.

[10]K. M. Muttaqi and M. T. Hagh, " A synchronization control technique for soft connection of doubly-fed induction generator based wind turbines to the power grid," in IEEE Industry Applications Society Annual Meeting, Cincinnati, OH, 2017, pp. 1-7.

[11]G. Tapia, G. Santamara, M. Telleria, and A. Susperregui. " Methodology for smooth connection of doubly fed induction generators to the grid", IEEE Trans. Energy Convers., vol.24, no.4, pp. 959-971, 2009.

[12] R. Pena, R. Cardenas, and G. Asher, "Overview of Control Systems for the Operation of DFIGs in Wind Energy Applications," in Annual Conference of the IEEE Industrial Electronics Society, Vienna, 2013, pp. 88–95.